Desalination 278 (2011) 173–178

Contents lists available at ScienceDirect

Desalination

journal homepage: www.elsevier.com/locate/desal

Effective photocatalytic disinfection of *E. coli* and *S. aureus* using polythiophene/MnO_2 nanocomposite photocatalyst under solar light irradiation

Kun Shang [a], Shiyun Ai [a,*], Qiang Ma [a], Tiantian Tang [b], Huanshun Yin [a], Haixiang Han [a]

[a] College of Chemistry and Material Science, Shandong Agricultural University, Taian, Shandong 271018, P.R. China
[b] College of Resources and Environment, Shandong Agricultural University, Taian, Shandong 271018, P.R. China

ARTICLE INFO

Article history:
Received 15 March 2011
Received in revised form 6 May 2011
Accepted 6 May 2011
Available online 28 May 2011

Keywords:
Photocatalytic disinfection
E. coli and *S. aureus*
PTh/MnO_2
Solar light
Hydroxyl radical

ABSTRACT

The photocatalytic disinfection of *Escherichia coli* (*E. coli*) and *Staphylococcus aureus* (*S. aureus*) was investigated systematically with polythiophene/MnO_2 (PTh/MnO_2) nanocomposite photocatalyst under solar light irradiation. The prepared PTh/MnO_2 nanocomposite was characterized by X-ray diffraction (XRD), transmission electron microscopy (TEM), Fourier transform infrared spectrum (FT-IR) and ultraviolet and visible absorption spectrum (UV-vis). The influence parameters of disinfection by PTh/MnO_2 nanocomposite, such as irradiation time and concentration of photocatalyst were studied. Further investigation indicated that almost all (99.9%) of the initial bacteria were killed after 6 h incubation at 37 °C in the presence of 1 mg/mL PTh/MnO_2 photocatalyst under solar light irradiation. During the photocatalytic process, the hydroxyl radical (·OH) was generated under irradiation, which played a key role in the inactivation of bacteria. The morphological change of the bacteria during the bactericidal process could be observed from TEM images. This work provides a potential effective nanocomposite photocatalyst to disinfect *E. coli* and *S. aureus* under solar light irradiation.

1. Introduction

Escherichia coli (*E. coli*) and *Staphylococcus aureus* (*S. aureus*) are highly infectious pathogens that commonly cause gastrointestinal illness and infectious diseases in humans, with potentially serious consequences [1,2]. Great interests in developing and implementing various materials and methods for the disinfection of pathogenic bacteria in water have been prompted with the increasing concern for public health and environmental quality. The traditional disinfectants methods, such as chlorine, ozone, chlorine dioxide and chloramines, may produce carcinogenic disinfection byproducts (DBPs) [3]. To reduce the formation of DBPs, it may be desirable to inactivate pathogens by environment-friendly disinfection methods.

The photocatalysis for water disinfection has got development in recent years. It has been reported for the first time that TiO_2 photocatalyst could kill bacterial cells in water by illumination, which could generate reactive oxygen species (ROS) in water medium [4]. Since then, numerous photocatalytic disinfection studies using TiO_2 photocatalyst have been reported [5–7]. However, TiO_2 only absorbs wavelengths in the near ultraviolet (UV) region (λ<400 nm), which is only about 3% of the solar spectrum, and it cannot efficiently utilize visible light [8]. Several approaches have been developed to extend the absorption band-edge of TiO_2 from UV to visible light region, including doping [9], sensitization [10], coating [11] and metallization [12]. However, the modifying processes are complex and the as-prepared samples are often suffered from the disadvantages such as low stability [13]. Thus, it is of great interest to develop photocatalysts that can yield high reactivity under solar light so that the solar spectrum may be maximally used to provide photocatalytic activity [14]. However, only a few studies are applied to the photocatalytic inactivation of pathogenic bacteria under solar light irradiation [15].

As a photoactive organic semiconductor, the polythiophene (PTh) has a wide absorption spectrum. Zhu et al. [16] reported the photocatalytic degradation of methyl orange by PTh/TiO_2 composites. Čík et al. [17] elucidated the photocatalytic bactericidal activity by photosensitizer PTh incorporated in ZSM-5 zeolite. Moreover, the surface defects play an important role in the photocatalytic activities. Doping metal oxide, such as MnO_2, can increase the surface defects. Jothiramalingam et al. studied the photocatalytic activity for toluene decomposition by manganese oxide doped TiO_2 [18]. All these efforts motivated us to dope PTh with MnO_2 to form polythiophene/MnO_2 (PTh/MnO_2) nanocomposite for the photocatalytic disinfection of bacteria under solar light. According to previous studies [12,19], we therefore assume that ·OH will be generated when PTh/MnO_2 photocatalyst are suspended in aqueous medium under solar light irradiation. In our previous work [20], it has been illustrated that ·OH can attack the cell membrane and wall, disrupt membrane integrity, or electrolyze the molecules in the cell surface, which brought massive cell kills and lyses.

* Corresponding author. Tel.: +86 538 8247660; fax: +86 538 8242251.
E-mail address: ashy@sdau.edu.cn (S. Ai).

0011-9164/$ – see front matter © 2011 Elsevier B.V. All rights reserved.
doi:10.1016/j.desal.2011.05.017

In this paper, PTh/MnO_2 nanocomposite was synthesized through interfacial polymerization. For the first time, the PTh/MnO_2 nanocomposite photocatalytic disinfection of pathogenic bacteria *E. coli* and *S. aureus* in sterilized river water under solar light irradiation was studied. The ·OH generated in photocatalytic process was determined through fluorescence methods [21]. The PTh/MnO_2 was proven to be a novel effective solar-light-driven bactericidal photocatalyst.

2. Experimental

2.1. Regents and materials

Thiophene and potassium permanganate were purchased from Jing Chun Chemical Co., Ltd. (Shanghai, China). Nutrient broth (NB) and Nutrient agar (NA) were obtained from Hope Bio-Technology Co., Ltd. (Qingdao, China). *E. coli* was selected from Gram-negative bacteria and *S. aureus* was selected from Gram-positive. Both bacterial genera were obtained from the College of Animal Science and Technology, Shandong Agricultural University (Taian, China). All other materials were of at least analytical grade and used without further purification. River water from the Nai River (Taian, China) was used after sterilization by autoclaving for 15 min at 121 °C at 0.1 Mpa and filtration through a membrane filter (0.22 μm pore-size). All aqueous solutions were prepared in deionized water.

2.2. Preparation and characterization of PTh/MnO_2 nanocomposite photocatalyst

PTh/MnO_2 nanocomposite photocatalyst was prepared by interfacial polymerization at 0 °C for 24 h [22]. 10 mL thiophene was dissolved in 300 mL CCl_4. 0.5 g potassium permanganate was dissolved in 300 mL distilled water (pH 7.0). In the reaction vial, the chemical oxidation polymerization of thiophene occurred at the aqueous/organic interface after mixing them with rigorous magnetic stirring. The reaction was in dark environment. After the reaction had finished the product was filtered. Then it was dispersed twice in the ethanol and five times in the distilled water to remove the excess of thiophene and potassium permanganate before being dried in vacuum dryer at 40 °C for 24 h.

Ultraviolet and visible absorption spectrums (UV-vis) of PTh/MnO_2, MnO_2 and PTh were obtained at 2450 UV-spectrophotometer (Shimazu, Japan). The spectrums were measured in the range of 200 to 750 nm. Fourier transform infrared spectrum (FT-IR) of PTh/MnO_2 was obtained at Nicolet 380 Fourier transform infrared spectrophotometer (Thermo, America). The spectrum was measured in the range of 400 to 4000 cm^{-1}. X-ray diffraction (XRD) pattern of PTh/MnO_2 was performed at D/MAX X-ray diffractometer (Rigaku, Japan) at the scanning rate of 4 min^{-1}. Transmission electron microscopy (TEM) images were obtained at 100CX II transmission electron microscope (JEM, Japan). All the characterizations were carried out at room temperature.

2.3. Culture of bacteria

Bacteria were cultured according to Chen et al. [20]. 50 μL of the *E. coli* suspension stored in glycerin was inoculated into 450 μL NB solution and cultured aerobically for 24 h at 37 °C with constant agitation. Then, 50 μL of the anabiotic *E. coli* suspension was inoculated into 450 μL NB at 37 °C for 4 h in order to reach the exponential growth phase. Finally, the suspension was immediately diluted into a certain number fold using NB solution and plated on NA plates using the spread plate method for counting. The stock suspension of *E. coli*, with the population varied from approximately 10^3 to 10^8 CFU/mL was prepared through the dilution of the counted *E. coli* suspension. The stock suspension of *S. aureus* was also prepared with the operations above.

2.4. Photocatalytic disinfection evaluation

The effects of PTh/MnO_2 photocatalyst on killing of *E. coli* and *S. aureus* were followed in two independent experiments. Firstly, the effect of different concentrations of PTh/MnO_2 on the growth of both bacterial species was studied under solar light irradiation (during the months of June to October in Taian (China) at around noon). 50 μL bacteria suspensions were inoculated in Erlenmeyer flask containing 100 mL of sterilized river water and an appropriate milligram of the PTh/MnO_2 photocatalyst. After 6 h incubation at 37 °C under solar light irradiation, the grown bacterial suspension was diluted and inoculated on NA in Petri dishes. After 24 h cultivation at 37 °C, the number of survived cells was counted. Secondly, the changes in survival rate of bacterial cells were obtained in dependence on the time of solar light irradiation. The second experiment was performed similarly to the first one, except that the suspension of bacteria grew in the presence of photocatalyst for a strictly determined time (1, 2, 3, 4, 5 and 6 h). At every time point the bacterial suspension was diluted and treated as described above. The survival ratio was defined as follows: Survival ratio $(\%) = (C_t/C_0) \times 100$, where C_0 and C_t are the numbers of surviving cells before photocatalysis and after photocatalysis, respectively. The antibacterial rate was defined as follows: Antibacterial rate $(\%) = 100 - \text{Survival ratio}$. The initial bacterial counts either for *E. coli* or for *S. aureus* was 5×10^3 CFU/mL. Sterilized river water was used to imitate the real river water that was suitable for the bacterial survival.

Additionally, the four control samples (with 1 mg/mL MnO_2 under irradiation, with 1 mg/mL PTh under irradiation, with 1 mg/mL PTh/MnO_2 in the dark and without PTh/MnO_2 under irradiation) were done under optimal conditions in order to determine the effectiveness of PTh/MnO_2 photocatalyst and the solar light irradiation. The number of surviving cells was calculated as a percentage in comparison with the no PTh/MnO_2 experiment (100%). In all the experiments, every sample was prepared in three parallels and the average values were given. All materials used in the experiments were autoclaved for 15 min at 121 °C at 0.1 Mpa.

2.5. Determination of hydroxyl radical

To confirm the conjecture that ·OH were generated when PTh/MnO_2 photocatalyst are suspended in water under solar light irradiation, the fluorescence methods were used to obtain information on the ·OH involved in experiment. 100 mg PTh/MnO_2 was added into the 100 mL solution containing 0.8 mmol/L cerous nitrate and 50 mmol/L sulfuric acid. The solution was irradiated with constant agitation at 37 °C under solar light. The supernatant of the mixture was tested once an hour using RF-5301PC fluorospectro photometer (Shimazu, Japan). Ce^{3+} can produce its characteristic fluorescence in diluted sulfuric acid with its excitation and emission wavelength at 280 nm and 360 nm, respectively. The fluorescence is quenched when Ce^{3+} is oxidized by ·OH ($Ce^{3+} + \cdot OH + H^+ \rightarrow Ce^{4+} + H_2O$). So the changes of fluorescence intensity can indicate the formation of ·OH [21]. Control experiments were carried out with 1 mg/mL PTh/MnO_2 in the dark and without PTh/MnO_2 under irradiation.

3. Results and discussion

3.1. Characterization of photocatalyst

Fig. 1A showed the powder XRD pattern of PTh/MnO_2. A broad diffraction peak was observed at around 37°, which may be related to the scattering from the PTh/MnO_2 [23]. The results of XRD analyses showed the low-crystalline tiny nanoparticles and the existence of amorphous polymers [24]. The amorphous state of the PTh/MnO_2 was principally attributed that the interplay between the formation of PTh and MnO_2 would hinder their crystallization. The XRD pattern of the

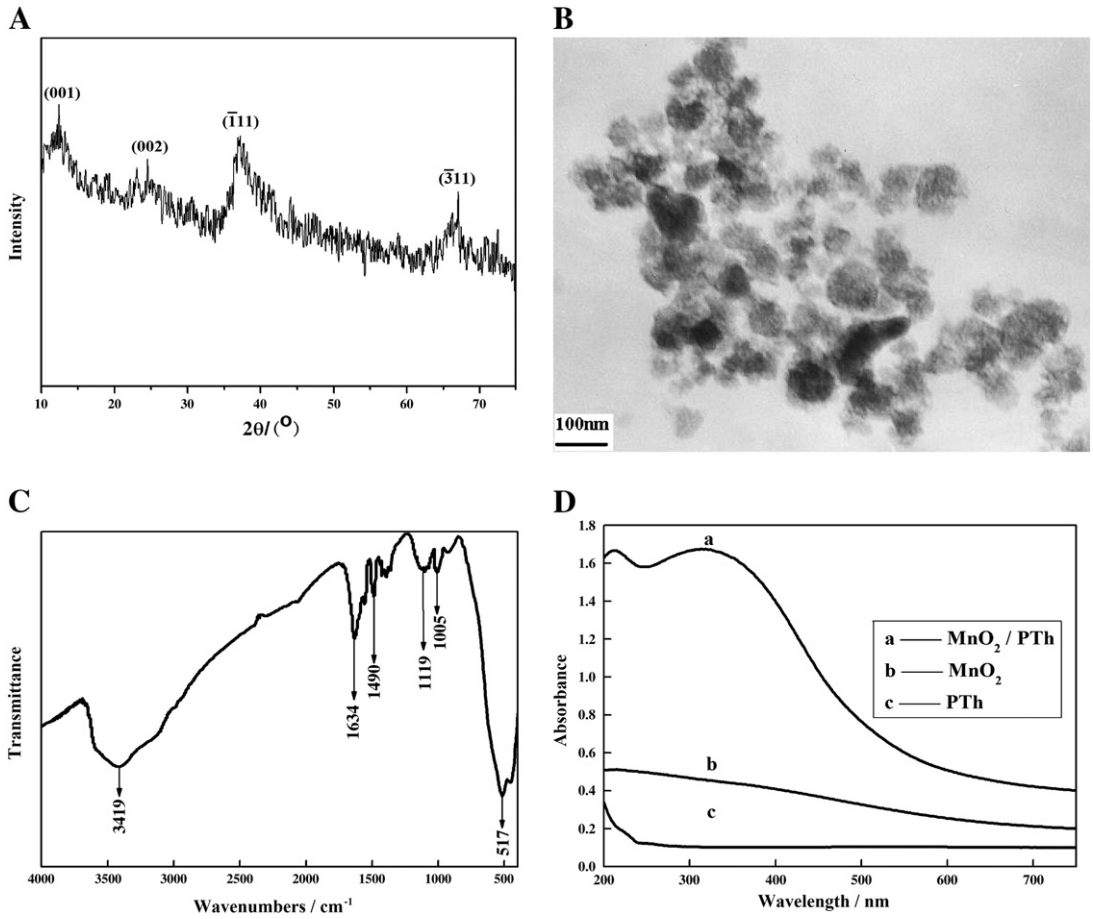

Fig. 1. (A) XRD pattern of PTh/MnO_2. (B) TEM image of PTh/MnO_2. (C) FT-IR spectrum of PTh/MnO_2. (D) UV-vis absorbance spectrum of PTh/MnO_2 (a), MnO_2 (b) and PTh (c).

sample confirmed the good thermal stability of PTh/MnO_2 as no distinct crystal phase formation was observed [25,26]. The TEM image of PTh/MnO_2 nanoparticles was shown in Fig. 1B. Irregular spheres were obtained. The particle sizes range was observed between 50 and 100 nm. Dozens of nanometer gaps existed between each PTh/MnO_2 particles. As shown in Fig. 1C, the FT-IR analysis confirmed the presences of PTh and MnO_2 in the product. The broad band in the regions from 400 to 600 cm^{-1} (517 cm^{-1}) can be attributed to Mn–O stretching vibrations, C_β–H out of plane bending vibration and deformation of thiophene ring. The characteristic band at 1005 cm^{-1} can be ascribed to C_β-H in the plane bending vibrations. The bands at 1490 cm^{-1} and 1119 cm^{-1} ban be attributed to C=C symmetric stretching vibrations of thiophene ring and C—C resonance absorption. The bands at 3419 cm^{-1} and 1634 cm^{-1} can be assigned to stretching and bending vibrations of the —OH group of crystal and adsorbed water molecules, respectively [22,25,27]. Therefore, the FT-IR confirmed the presence of PTh and MnO_2 in the composite. Fig. 1D showed the different UV-vis absorbance spectra of PTh/MnO_2 (a), MnO_2 (b) and PTh (c) with the same concentration. The absorption of PTh/MnO_2 nanocomposite was much stronger than MnO_2 and PTh. The shape of the spectrum (a) demonstrated that it was possible to prepare PTh/MnO_2 with effective absorption of light from 200 up to 750 nm by interfacial polymerization of thiophene with potassium permanganate. Therefore, effective excitation of PTh/MnO_2 will occur by illumination.

3.2. Photocatalytic disinfection performance

The effect of different irradiation time on the antibacterial rate, from 0 to 8 h, was studied (Fig. 2A). The antibacterial rate of photocatalyst increased when the irradiation time prolonged. For example, the antibacterial rate against *E. coli* with the irradiation time of 1, 2, 3 and 4 h were 13.2%, 27.5%, 57.9% and 91.1%, respectively. PTh/MnO_2 photocatalyst exhibited a low bactericidal activity at the initial stage (the first 3 h) of photocatalytic process. However, the antibacterial rates rapidly increased in excess of 90% after 4 h of irradiation. Almost all (99.9%) of the initial bacteria were inactivated in the presence of 1.0 mg/mL PTh/MnO_2 photocatalyst after 6 h of solar light irradiation. Hence, 6 h was chosen as the optimal irradiation time. In order to understand the effect of photocatalyst concentration on inactivation, we have conducted experiments with different concentration of PTh/MnO_2 under solar light and the results were illustrated in Fig. 2B. The antibacterial rate of PTh/MnO_2 against *E. coli* and *S. aureus* increased with the increasing concentration of photocatalyst. For example, the antibacterial rate against *E. coli* with the concentration of 0.1, 0.25, 0.5 and 0.75 mg/mL were 93.8%, 94.2%, 95.4% and 99.4%, respectively. The antibacterial rate achieved 99.9% when the concentration of PTh/MnO_2 was 1.0 mg/mL. The almost unchanged antibacterial rates above 1.0 mg/mL, in Fig. 2B, can be attributed to the saturating concentration of PTh/MnO_2 photocatalyst. The saturating photoactivity with increasing PTh/MnO_2 concentration could be explained by the competition between the light scattering loss and the surface area [13]. Due to the increased light scattering, the light penetration depth into the suspension decreases when PTh/MnO_2 with higher concentration provides more active catalytic sites [28]. Therefore, the photocatalyst concentration of 1.0 mg/mL was chosen for the optimum concentration. The results indicated that both irradiation time and photocatalyst concentration had effects on the photocatalytic disinfection performance. This was mainly attributed to the increasing amount of ·OH generated during the photocatalytic process [29].

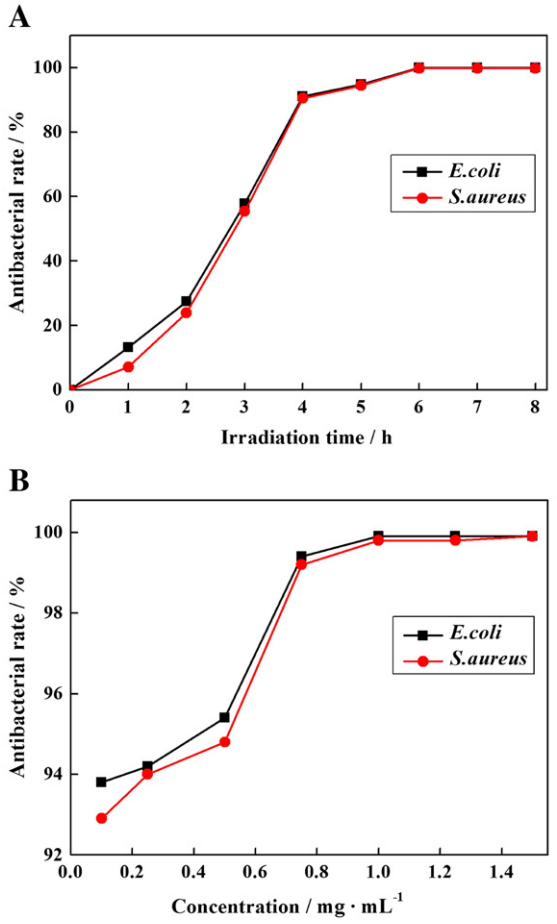

Fig. 2. The antibacterial rates on the irradiation time (1 mg/mL PTh/MnO_2) (A) and the concentration of photocatalyst (t_{exp} = 6 h) (B).

However, from the results of Fig. 2, *E. coli* was more sensitive than *S. aureus* during photocatalytic process. The discrepancies in susceptibility of both bacterial species to the PTh/MnO_2 photocatalyst can be attributed to the different cell wall structures, chemical compositions, biological forms, biological reactions and sensibilities of Gram-positive and Gram-negative bacteria [17].

The first two control experiments, without the PTh/MnO_2 under irradiation and with PTh/MnO_2 in the dark, did not show any bactericidal effects on *E. coli* and *S. aureus* (Fig. 3), which indicated

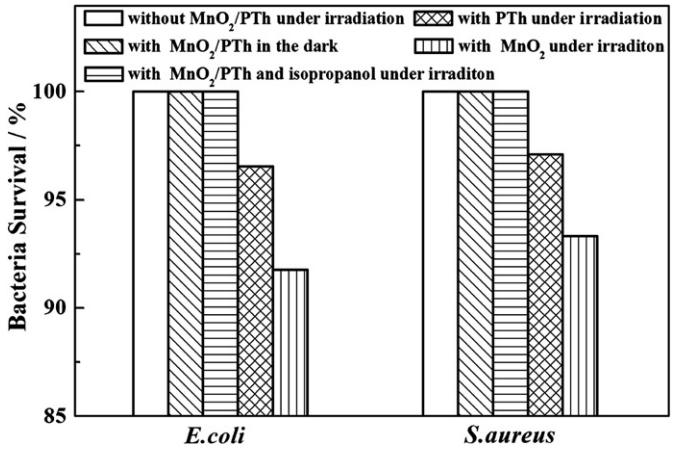

Fig. 3. The antibacterial efficiency of the control experiments (t_{exp} = 6 h).

that the photocatalyst itself was not toxic to the bacteria [30]. Thus, the bactericidal effect on bacteria was undoubtedly ascribed to the photocatalytic reaction of the PTh/MnO_2 under solar light irradiation. As shown in Fig. 3, MnO_2 and PTh had weak bactericidal effects under irradiation, which were in sharp contrast with the effect of PTh/MnO_2 photocatalyst. It was consistent with the ability of absorption that resulted from the UV-vis absorbance spectrums. Furthermore, the reclaimed PTh/MnO_2 exhibited the same antibacterial efficiency (date were not shown) compared with the freshly prepared PTh/MnO_2 photocatalyst. Therefore, PTh/MnO_2 photocatalyst can be recycled, which save the resources effectively. It also showed the PTh/MnO_2 photocatalyst had good stability in photocatalytic process.

We also invested the antibacterial rates on varying initial bacterial counts at optimum conditions. The suspension of bacterial, with the population varied from 10^2 to 10^6 CFU/mL, was irradiated for 6 h under solar light with the 1.0 mg/mL PTh/MnO_2. The results were listed in Table 1. All the samples showed a similar antibacterial rate (approximate to 99.9%), revealing that this method is effective and reliable.

3.3. Photocatalytic disinfection mechanism

As shown in Fig. 4A, the nearly unchanged relative intensity of fluorescence demonstrated that few ·OH was generated without PTh/MnO_2 under irradiation (I) and with PTh/MnO_2 in the dark (II). However the significant change was observed with PTh/MnO_2 under irradiation in Fig. 4A (III), indicating that a large number of ·OH formed during irradiation for 6 h under solar light [21]. Fig. 4B showed the relative intensity of fluorescence with 1 mg/mL PTh/MnO_2 under solar light irradiation at every time point. With extending the time (curves a to g), the increasing amount of generated ·OH during irradiation led to the decrease of the relative intensity of fluorescence, which was in accordance with Fig. 4A (III).

Isopropanol (0.3 mol/L) was employed as a diagnostic tool for the ·OH to clarify whether the photocatalytic disinfection of *E. coli* and *S. aureus* was caused by ·OH because isopropanol was easily oxidized by ·OH and has low effect on semiconductor surfaces in aqueous medium [31]. As expected, as can be seen from Fig. 3, the photocatalytic disinfection of bacteria could be completely inhibited by the addition of isopropanol, which indicated that the ·OH played an important role during in photocatalytic process in the aqueous suspension. The ·OH has oxidizing potentials higher than that of chlorine or even ozone [32,33]. A significant disorder in the cell permeability and the decomposition of the cell walls and DNA damage is caused by ·OH [13,34].

To understand the destruction process of bacteria by the ·OH generated by PTh/MnO_2 photocatalyst, the morphology and structure of bacteria at the different stages of photocatalytic process were examined by TEM studies (Fig. 5). Fig. 5A showed the appearance of *E. coli* before reaction. The characteristic shape of untreated *E. coli* indicated that the bacteria were in a normal condition without environment disturbance [19]. After the *E. coli* suspension was irradiated by solar light for 6 h with 1.0 mg/mL PTh/MnO_2 photocatalyst, extremely obvious changes were observed in the cells. The cell wall was torn in places and the cytoplasm had leak to the external environment (Fig. 5B). This observation was well matched with the previous study that significant disorder in membrane permeability can be caused by the attack of photogenerated ·OH [31]. A same destruction process was observed in *S. aureus*

Table 1
The antibacterial rates on varying initial bacterial counts (1 mg/mL PTh/MnO_2, t_{exp} = 6 h).

Initial bacterial counts/CFU·mL^{-1}	10^2	10^3	10^4	10^5	10^6
Antibacterial rate (*E. coli*)/%	99.93	99.92	99.93	99.92	99.92
Antibacterial rate (*S. aureus*)/%	99.91	99.92	99.91	99.92	99.91

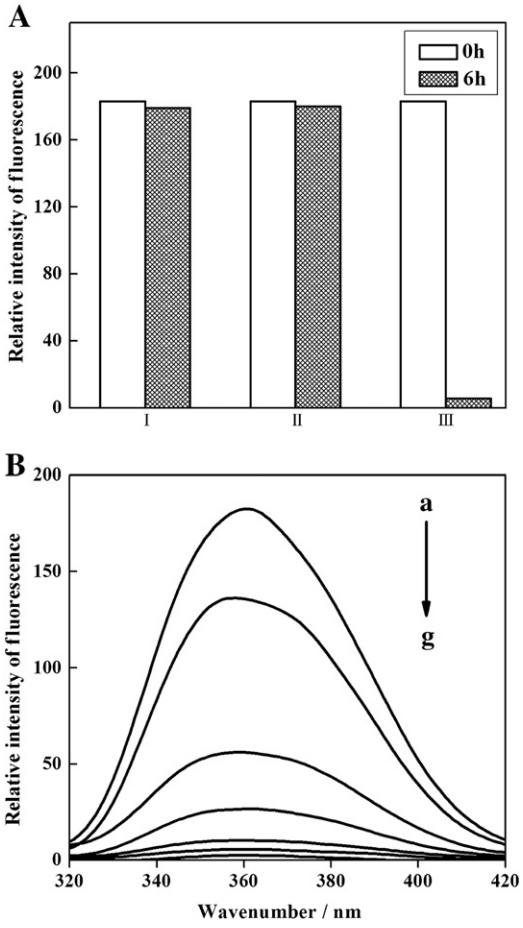

Fig. 4. (A) The relative intensity of fluorescence of the supernatant before and after experiments (treated for 6 h) under different conditions: without PTh/MnO_2 under irradiation (I); with 1 mg/mL PTh/MnO_2 in the dark (II); with 1 mg/mL PTh/MnO_2 under irradiation (III). (B) The relative intensity of fluorescence from 0 to 6 h (curves a to g) with 1 mg/mL PTh/MnO_2 under irradiation.

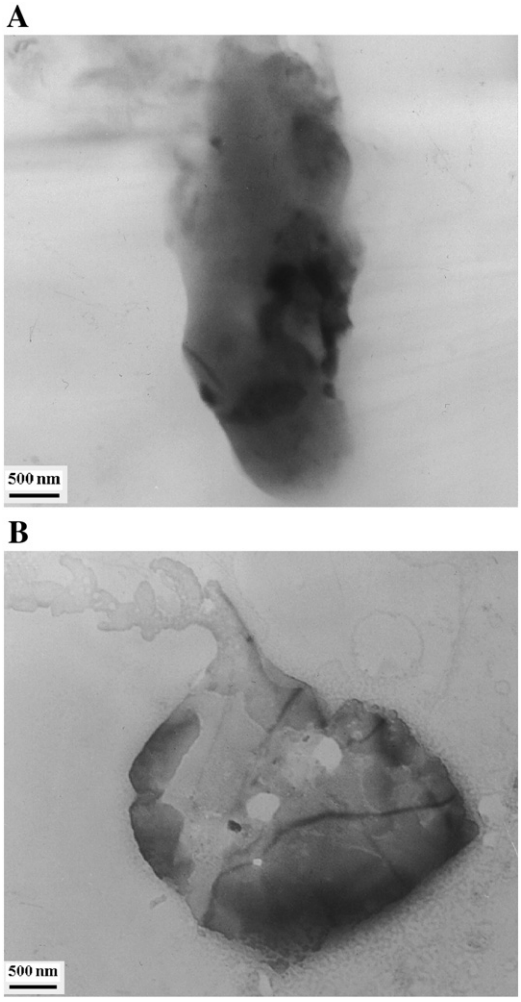

Fig. 5. TEM images of *E. coli* photocatalytically untreated or treated with PTh/MnO_2 photocatalyst under solar light irradiation. (A) Before irradiation, (B) After irradiated with PTh/MnO_2 for 6 h.

suspension as well (images were not shown). These results suggested that the bacteria were damaged in the presence of PTh/MnO_2 under the solar light irradiation. The PTh/MnO_2 photocatalyst could decompose the cell wall and the cell membrane by ·OH. The photocatalytic process increased the cell permeability and subsequently allowed free efflux of intracellular constituents, which eventually lead to the cell death [8,13].

4. Conclusion

In summary, we reported interfacial polymerization for synthesis of PTh/MnO_2 nanocomposite photocatalyst. PTh/MnO_2 showed an amorphous structure and the particle size was in the range of 50 to 100 nm. The prepared PTh/MnO_2 nanocomposite photocatalyst effectively absorbed the solar energy and exhibited a remarkable solar-light-induced photocatalytic antibacterial capability due to the ·OH that generated during photocatalytic process. The ·OH generated under solar light irradiation was determined by fluorescence methods. The generation of ·OH is the major lethal species responsible for the photocatalytic disinfection. Photocatalytic disinfection tests showed that the antibacterial rates could achieve up to 99.9% after 6 h irradiation of solar light with 1 mg/mL PTh/MnO_2 photocatalyst. Thus there is a new possibility of application of PTh/MnO_2 photocatalyst in the protection of biologically contaminated environment and other related areas.

Acknowledgments

This work was supported by the National Natural Science Foundation of China (No. 21075078) and the Natural Science Foundation of Shandong province, China (No. ZR2010BM005).

References

[1] Y. Tsai, P. Cheng, T. Pan, Immunomodulating activity of *Lactobacillus paracasei* subsp. *paracasei* NTU 101 in enterohemorrhagic *Escherichia coli* O157H7-infected mice, J. Agric. Food Chem. 58 (2010) 1207–1212.
[2] W. Chang, F. Toghrol, W.E. Bentley, Toxicogenomic response of *Staphylococcus aureus* to peracetic acid, Environ. Sci. Technol. 40 (2006) 5124–5131.
[3] C. Hu, X. Hu, J. Guo, J. Qu, Efficient destruction of pathogenic bacteria with NiO/$SrBi_2O_4$ under visible light irradiation, Environ. Sci. Technol. 40 (2006) 5508–5513.
[4] T. Matsunaga, R. Tomoda, T. Nakajima, H. Wake, Photoelectrochemical sterilization of microbial cells by semiconductor powders, FEMS Microbiol. Lett. 29 (1985) 211–214.
[5] C. Wei, W.Y. Lin, Z. Zainal, N.E. Williams, K. Zhu, A.P. Kruzic, R.L. Smith, K. Rajeshwar, Bactericidal activity of TiO_2 photocatalyst in aqueous media: toward a solar-assisted water disinfection system, Environ. Sci. Technol. 28 (1994) 934–938.
[6] K. Sunada, Y. Kikuchi, K. Hashimoto, A. Fujishima, Bactericidal and detoxification effects of TiO_2 thin Film photocatalysts, Environ. Sci. Technol. 32 (1998) 726–728.
[7] C.A. Linkous, G.J. Carter, D.B. Locuson, A.J. Ouellette, D.K. Slattery, L.A. Smitha, Photocatalytic inhibition of algae growth using TiO_2, WO_3, and cocatalyst modifications, Environ. Sci. Technol. 34 (2000) 4754–4758.
[8] C. Hu, J. Guo, J. Qu, X. Hu, Photocatalytic degradation of pathogenic bacteria with AgI/TiO_2 under visible light irradiation, Langmuir 23 (2007) 4982–4987.
[9] R. Asahi, T. Morikawa, T. Ohwaki, K. Aoki, Y. Taga, Visible-light photocatalysis in nitrogen-doped titanium oxides, Science 293 (2001) 269–271.

[10] M. Zhang, C. Chen, W. Ma, J. Zhao, Visible-light-induced aerobic oxidation of alcohols in a coupled photocatalytic system of dye-sensitized TiO_2 and TEMPO, Angew. Chem. Int. Ed. 47 (2008) 9730–9733.
[11] R.W. Fessenden, P.V. Kamat, Rate constants for charge injection from excited sensitizer into SnO_2, ZnO, and TiO_2 semiconductor nanocrystallites, J. Phys. Chem. 99 (1995) 12902–12906.
[12] M.R. Elahifard, S. Rahimnejad, S. Haghighi, M.R. Gholami, Apatite-coated Ag/AgBr/TiO_2 visible-light photocatalyst for destruction of bacteria, J. Am. Chem. Soc. 129 (2007) 9552–9553.
[13] J. Ren, W. Wang, L. Zhang, J. Chang, S. Hu, Photocatalytic inactivation of bacteria by photocatalyst Bi_2WO_6 under visible light, Catal. Commun. 10 (2009) 1940–1943.
[14] P. Wang, B. Huang, X. Qin, X. Zhang, Y. Dai, M.-H. Whangbo, Ag/AgBr/$WO_3 \cdot H_2O$: visible-light photocatalyst for bacteria destruction, Inorg. Chem. 48 (2009) 10697–10702.
[15] O. Akhavan, E. Ghaderi, Photocatalytic reduction of graphene oxide nanosheets on TiO_2 thin film for photoinactivation of bacteria in solar light irradiation, J. Phys. Chem. C 113 (2009) 20214–20220.
[16] Y. Zhu, S. Xu, D. Yi, Photocatalytic degradation of methyl orange using polythiophene/titanium dioxide composites, React. Funct. Polym. 70 (2010) 282–287.
[17] G. Čík, S. Priesolová, H. Bujdáková, F. Sersen, T. Potheöová, J. Kristín, Inactivation of bacteria G^+-*S. aureus* and G^--*E. coli* by phototoxic polythiophene incorporated in ZSM-5 zeolite, Chemosphere 63 (2006) 1419–1426.
[18] R. Jothiramalingam, M.K. Wang, Synthesis, characterization and photocatalytic activity of porous manganese oxide doped titania for toluene decomposition, J. Hazard. Mater. 147 (2007) 562–569.
[19] C. Hu, Y. Lan, J. Qu, X. Hu, A. Wang, Ag/AgBr/TiO_2 visible light photocatalyst for destruction of azodyes and bacteria, J. Phys. Chem. B 110 (2006) 4066–4072.
[20] Q. Chen, S. Ai, S. Li, J. Xu, H. Yin, Q. Ma, Facile preparation of PbO_2 electrode for the electrochemical inactivation of microorganisms, Electrochem. Commun. 11 (2009) 2233–2236.
[21] C. Li, G. Song, Photocatalytic degradation of organic pollutants and detection of chemical oxygen demand by fluorescence methods, Sens. Actuators B 137 (2009) 432–436.
[22] Y.G. Wang, W. Wu, L. Cheng, P. He, C.X. Wang, Y.Y. Xia, A polyaniline-intercalated layered manganese oxide nanocomposite prepared by an inorganic/organic interface reaction and its high electrochemical performance for Li storage, Adv. Mater. (Weinheim, Ger.) 20 (2008) 2166–2170.
[23] Q. Lu, Y. Zhou, Synthesis of mesoporous polythiophene/MnO_2 nanocomposite and its enhanced pseudocapacitive properties, J. Power Sources 196 (2011) 4088–4094.
[24] W. Xiao, J.S. Chen, Q. Lu, X.W. Lou, Porous spheres assembled from polythiophene (PTh)-coated ultrathin MnO_2 nanosheets with enhanced lithium storage capabilities, J. Phys. Chem. C 114 (2010) 12048–12051.
[25] X.-G. Li, J. Li, M.-R. Huang, Facile optimal synthesis of inherently electroconductive polythiophene nanoparticles, Chem. Eur. J. 15 (2009) 6446–6455.
[26] F. Wang, S. Arai, M. Endo, The preparation of multi-walled carbon nanotubes with a Ni-P coating by an electroless deposition process, Carbon 43 (2005) 1716–1721.
[27] H. Meng, D. Perepichka, M. Bendikov, F. Wudl, G. Pan, W. Yu, W. Dong, S. Brown, Solid-state synthesis of a conducting polythiophene via an unprecedented heterocyclic coupling reaction, J. Am. Chem. Soc. 125 (2003) 15151–15162.
[28] M. Bekbölet, Photocatalytic bactericidal activity of TiO_2 in aqueous suspensions of *E. coli*, Water Sci. Technol. 35 (1997) 95–100.
[29] S. Xu, Y. Zhu, L. Jiang, Y. Dan, Visible light induced photocatalytic degradation of methyl orange by polythiophene/TiO_2 composite particles, Water Air Soil Pollut. 213 (2010) 151–159.
[30] J.C. Yu, W. Ho, J. Yu, H. Yip, P.K. Wong, J. Zhao, Efficient visible-light-induced photocatalytic disinfection on sulfur-doped nanocrystalline titania, Environ. Sci. Technol. 39 (2005) 1175–1179.
[31] L.-S. Zhang, K.-H. Wong, H.-Y. Yip, C. Hu, J.C. Yu, C.-Y. Chan, P.-K. Wong, Effective photocatalytic disinfection of *E. coli* K-12 using $AgBr-Ag-Bi_2WO_6$ nanojunction system irradiated by visible light: the role of diffusing hydroxyl radicals, Environ. Sci. Technol. 44 (2010) 1392–1398.
[32] K.T. Kawagoe, D.C. Johnson, Electrocatalysis of anodic oxygen-transfer reactions, J. Electrochem. Soc. 141 (1994) 3404–3409.
[33] N. Yu, L. Gao, S. Zhao, Z. Wang, Electrodeposited PbO_2 thin film as positive electrode in PbO_2/AC hybrid capacitor, Electrochim. Acta 54 (2009) 3835–3841.
[34] G.K. Prasad, P.V.R.K. Ramacharyulu, S. Merwyn, G.S. Agarwal, A.R. Srivastava, B. Singh, G.P. Rai, R. Vijayaraghavan, Photocatalytic inactivation of spores of *Bacillus anthracis* using titania nanomaterials, J. Hazard. Mater. 185 (2011) 977–982.